

# Preparation and Characterization of Chitosan Based Micro Networks: Transposition to a Prilling Process

L. Martinez,<sup>1</sup> F. Agnely,<sup>1</sup> R. Bettini,<sup>2</sup> M. Besnard,<sup>1</sup> P. Colombo,<sup>2</sup> G. Couarraze<sup>1</sup>

<sup>1</sup>Laboratoire de Physique Pharmaceutique UMR CNRS 8612, Faculté de Pharmacie de l'Université Paris-Sud, 5 rue J.-B. Clément, 92296 Châtenay-Malabry Cedex, France

<sup>2</sup>Dipartimento Farmaceutico, Facoltà di Farmacia, Università degli Studi di Parma, Parco Area delle Scienze, 43100 Parma, Italy

Received 30 October 2003; accepted 19 March 2004

DOI 10.1002/app.20785

Published online in Wiley InterScience (www.interscience.wiley.com).

**ABSTRACT:** Beads of chitosan (CS) crosslinked network and of chitosan/poly(ethylene oxide) (CS/PEO) semi-interpenetrating network (semi-IPN) were prepared by a dropping technique and characterized. PEO content in the beads of semi-IPN was determined by gel permeation chromatography. CS crosslinking ratio was evaluated qualitatively by ATR-FTIR spectroscopy and quantitatively by UV spectrophotometry. After drying in a fluidized bed apparatus, a monodisperse population of well individualized, spherical, and smooth particles was obtained. It was shown that bead collapse during the drying stage was avoided thanks to the chemical crosslinking of CS chains. By the prilling, or laminar jet break-up technology, production at a larger scale

was also achieved. This process allowed the formation of a row of well calibrated drops of polymer solution under the influence of a vibration. Polymer solution characteristics, particularly viscosity, constituted a critical factor in the feasibility of the prilling process. Transposition of the formulation was managed through the optimization of process parameters such as vibration frequency, amplitude, and flow rate. © 2004 Wiley Periodicals, Inc. *J Appl Polym Sci* 93: 2550–2558, 2004

**Key words:** chitosan; semi-IPN; crosslinking; prilling process; particle size distribution

## INTRODUCTION

CS is a natural and abundant polysaccharide obtained by *N*-deacetylation of chitin. Chitin is an extracted product of crustaceans' and insects' shell, algae, and some kinds of fungi (Fig. 1). The physicochemical and biological properties of CS, such as biodegradability, biocompatibility, and non toxicity, are of great interest in the biomedical and pharmaceutical fields.<sup>1–6</sup> Thanks to their pH-dependent swelling properties, CS networks are already used as hydrophilic matrices for the controlled delivery of drugs.<sup>7,8</sup>

Recently, CS/PEO semi-IPN were developed.<sup>9–11</sup> They consist of the two polymers CS and PEO linked together by physical bonds, while CS chains are linked in a covalent way by means of a crosslinking agent. Entrapped PEO chains increase the swelling ability and reinforce the mechanical properties of the CS reference network.<sup>10</sup>

Meanwhile, trends in pharmaceutical processing have turned towards the design of increasingly high quality particles, that is, monosized, spherical, and free-flowing particles. Indeed, variable size distribu-

tions and heterogeneous shapes are detrimental to an efficient processing. The use of small and spherical particles with uniform size allows overcoming the disadvantages that could result from the use of raw powders and granulates.

The crushing of CS is quite difficult and leads to particles of very heterogeneous shape. That is why a direct synthesis in a divided form would represent a mean to get fine and free flowing particles more easily. The purpose of this work focused on the preparation of beads of CS network and of CS/PEO semi-IPN.

## METHODS

### Materials and sample preparation

CS from crab shells was purchased from Sigma<sup>®</sup> (Steinheim, Germany). Its average deacetylation degree, determined by IR spectroscopy on Impact 420 Nicolet FTIR spectrometer (Nicolet Instrument Corp., Madison, WI) according to Brugnerotto et al. method, was 83%.<sup>12</sup> Its average molar mass, measured by Ubbelohde capillary viscometry on AVS 400 viscometer (Schott-Geräte GmbH, Hofheim, Germany), was 1,600,000 g/mol.<sup>13</sup> PEO 1,000,000 g/mol (manufacturer's specifications) was supplied by Aldrich<sup>®</sup> (Milwaukee, WI). Glyoxal was used as the crosslinking agent. A 40% glyoxal aqueous solution was provided

Correspondence to: L. Martinez (leticia.martinez@cep.u-psud.fr).

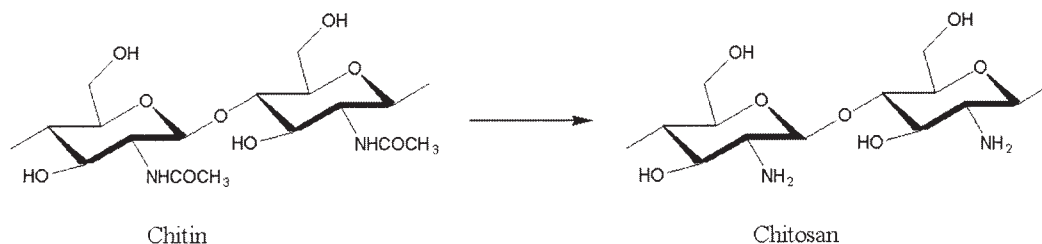


Figure 1 Chitin and chitosan molecules.

by Acros Organics (Loughborough, UK). All other reagents used in the experiments were of analytical grade.

It is worth noting that CS moisture content (10%, determined by thermogravimetric analysis on Perkin-Elmer TGA7, Perkin-Elmer Instruments, Boston, MA) was taken into account for the calculation of polymer concentrations. CS was solubilized in 2%(w/v) acetic acid aqueous solution to a concentration of 1.5%(w/w) under gentle stirring for a night. Afterwards, the solution was filtered on Whatman ashless filter paper (Whatman Limited, Maidstone, UK). To form the semi-IPN, PEO was added to the CS solution to a ratio of 20%(w/w) in relation to the weight of dried CS.<sup>10</sup> The reference CS solution was prepared in the same way, but without addition of PEO.

In a first step, beads were obtained by dropping the polymer solution into a proper reception bath. Second, to lead the production at a larger scale, the formulation was transposed to a prilling process.

Technical and formulation parameters were evaluated to optimize synthesis process of those micro networks. The beads obtained in both processes were characterized by their size distribution, true density, and specific surface area.

### Beads preparation

Polymer solutions were dropped into 10%(w/v) sodium hydroxide solution through a flat-tip needle with an internal diameter of 450  $\mu\text{m}$ , by means of a peristaltic pump at a rate of 1 mL/min. The solutions were divided by this way into calibrated drops. Since CS is a cationic polymer with ammonium groups, drops could be solidified by precipitation of the polymer. Thus, beads were collected and washed with distilled water to remove residual sodium hydroxide, until the solution they were suspended in recovered neutrality.

At this stage of the preparation, to determine the amount of PEO remaining within the semi-IPN after the process, the concentration of PEO in the precipitating solution was quantified by gel permeation chromatography (Ultrahydrogel<sup>TM</sup> 250 column 7.8  $\times$  300 mm/6  $\mu\text{m}$ , Waters Corp., Milford, MA; HPLC Waters 501 pump, Waters 712 WISP injector, Waters 484 Tunable UV detector, and Waters 745 Data Module inte-

grator, Millipore Waters Chromatography Division, Milford, MA; mobile phase NaCl 0.1N, flow rate: 1 mL/min, injection volume: 100  $\mu\text{L}$ , wavelength: 220 nm).

To form a covalent network, CS chains were crosslinked with glyoxal. Crosslinked chitosan is noted G in the text. As a dialdehyde molecule, glyoxal reacted with CS to form a Schiff base between CS amine groups and glyoxal aldehyde functions.<sup>14,15</sup> The crosslinking solution was prepared so that glyoxal concentration corresponded to the stoichiometric molar ratio in relation to CS amine groups, assuming that 1 molecule of glyoxal reacts with 2 units of CS.<sup>15</sup> The stoichiometric molar ratio [glyoxal : amine group] is noted 0.5 : 1. Thus, 20 g of the above beads were suspended in 250 mL of a 3 mM glyoxal aqueous solution. Beads were submitted to crosslinking reaction at room temperature for 24 h under stirring. After 24 h, the amount of glyoxal remaining in the surrounding solution was measured by UV spectroscopy at 322 nm on Beckman DU-70 spectrophotometer (Beckman Coulter, Inc., Fullerton, CA) according to the procedure reported by Mitchel and Birnboim.<sup>16</sup> Then, the amount of glyoxal that diffused into the beads could be deduced by subtraction. Afterwards, beads were transferred into 250 mL of distilled water under stirring for another 24 h. The amount of glyoxal released from the beads was assumed to correspond to unbound reactive and was determined again. Those two successive determinations gave by deduction the amount of glyoxal that actually remained in the beads and did react with CS.

A qualitative analysis of the crosslinking reaction was performed by attenuated total reflectance infrared spectroscopy. It was conducted on Impact 420 Nicolet FTIR spectrometer (Madison, WI) equipped with a horizontal ATR accessory (HATR). Dried beads were placed onto the diamond crystal and pressed for an intimate contact. Transmission spectra were collected with 64 scans and a resolution of 2  $\text{cm}^{-1}$ .

### Drying process

After the crosslinking step, beads were dried in a fluidized bed apparatus (Aeromatic-Fielder AG, Bubendorf, Switzerland). Process conditions are given

below: the chamber of the Aeromatic was loaded with 60 g of beads; inlet and outlet temperatures were 38°C and 36°C, respectively; air volume was 2 m<sup>3</sup>/min. Compressed air was also injected through a nozzle by the top of the chamber to disperse the beads easily: a pressure of 2 bars was applied for the first 15 min, then 1 bar was maintained for the rest of the time. Drying was performed in 1 h.

### Particle size distribution and textural characterization

Particle size distribution was determined by laser diffraction on Coulter LS 230 apparatus (Beckman Coulter, Inc., Miami, FL). Beads were dispersed in 1/1 (v/v) silicon oil 47V20/tetrachloroethane (density of 1.3 g/mL). This solvent was found convenient for avoiding bead sedimentation and swelling.

The B.E.T. method (Coulter SA 3100, Beckman Coulter, Inc., Miami, FL) allowed the measurement of beads' specific surface area using krypton as the adsorbing gas at the temperature of liquid nitrogen.

True density, determined by helium pycnometry, was carried out on Accupyc 1330 pycnometer (Micromeritics, Norcross, GA). Beads' shape and surface was also assessed using scanning electron microscopy (LEO 1530 Gemini, LEO Electron Microscopy Ltd, Cambridge, UK) with 3 nm Au/Pd coating, 3 keV energy, and a magnification of 100 and 1000 for shape and surface, respectively.

### Transposition to a prilling device

The prilling process is a method for producing particles with tailored properties, uniform spherical geometry, and narrow particle size distribution.<sup>17-19</sup> It works on the principle of "laminar jet break-up"; under the influence of a vibration whose wavelength is longer than the girth of the undisturbed jet, the laminar liquid jet breaks apart into a chain of drops.<sup>20</sup> To

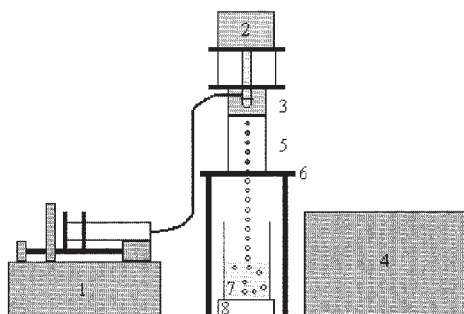


**Figure 2** Components of the prilling device: (1) Syringe pump; (2) Vibration unit; (3) Head with single nozzle; (4) Control cabinet; (5) Stroboscopic light; (6) Support for the head; (7) Hardening solution with beads; (8) Laboratory stirrer

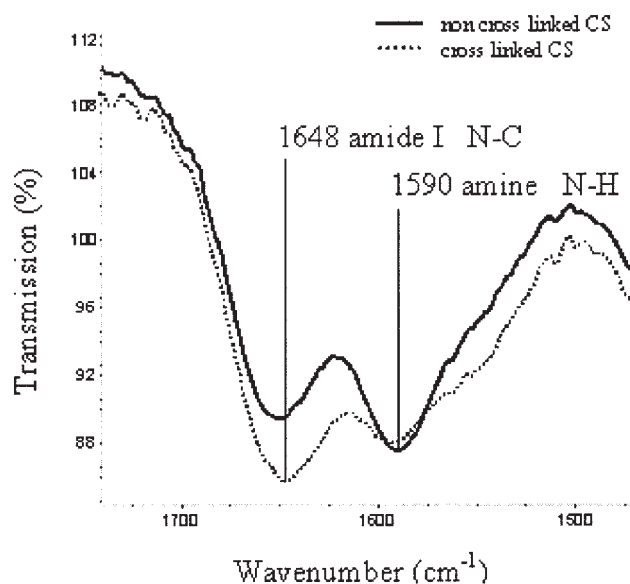


**Figure 3** IR spectra of non crosslinked and crosslinked chitosan: inversion of the amide/amine intensity ratio.

superimpose the vibration, the nozzle itself is vibrated. Constant flow and vibration result into mono-sized drops. The surface tension of these droplets molds them into spheres; then, their solidification is induced in gaseous medium through cooling or drying and/or in liquid medium through chemical reaction. Final particles are called prills.

The device used in these experiments was the Nisco Encapsulation Unit VAR D (Nisco Engineering Inc, Zurich, Switzerland). The unit consisted of the following modular components (Fig. 2):

- an electromagnetic vibrator,
- a head with sight glass to observe the drops,
- a syringe pump with a 70 mL syringe,
- a control cabinet (to fix vibration frequency, amplitude, and LED intensity), and
- a 200  $\mu$ m stainless steel nozzle.

### Formulation and process parameters

Polymer solutions were pumped through the vibrating nozzle system where, upon exiting, the liquid

**TABLE I**  
Effective [glyoxal:amine group] Molar Ratio and Calculated Cross-Linking Density ( $M_C$ ) for Crosslinked CS (CS1.5% G) and Semi-IPN (CS1.5% G PEO) Beads Obtained by the Non-Vibrating Dropping Process (mean  $\pm$  S.D.)

	CS1.5% G	CS1.5% G PEO
Theoretical molar ratio	0.5 : 1	0.5 : 1
Reacting glyoxal (%)	39 $\pm$ 4	40 $\pm$ 2
Effective molar ratio	0.19 : 1	0.20 : 1
$M_C$ (g/mol)	640 $\pm$ 120	620 $\pm$ 60

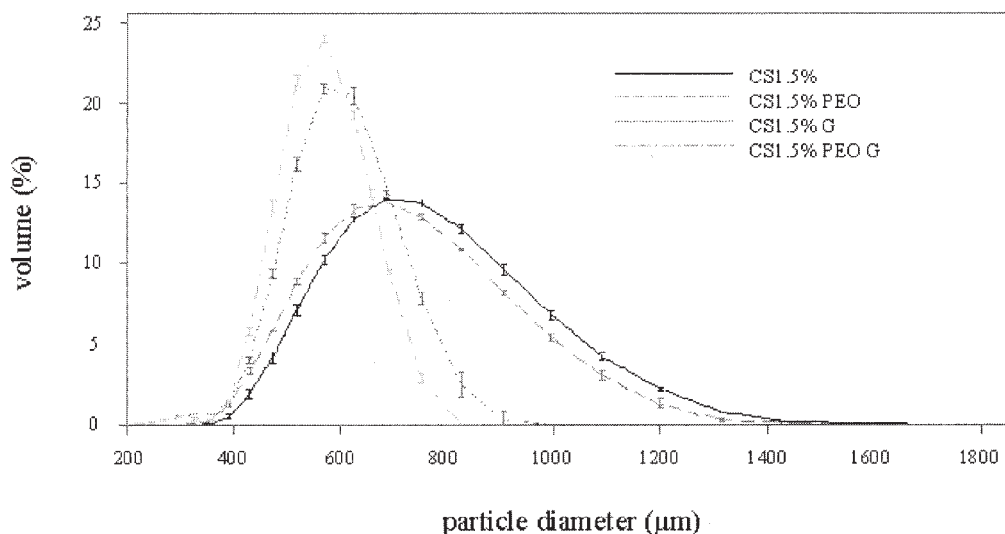


**Figure 4** Particle size distribution for CS1.5% and CS1.5% PEO dried beads whether chitosan is crosslinked or not. G indicates a crosslinked chitosan.

stream broke apart into uniform droplets. These droplets were solidified in 10%(w/v) sodium hydroxide solution. To fit the technique to the material, some parameters of the process such as vibration frequency, amplitude, and flow rate, as well as some aspects of the previous formulations, were optimized in the study.

The viscosity of CS and CS/PEO solutions was determined on Carrimed CSL 100 rheometer (Rheo, Champlan, France). Measurements were realized with a cone/plate geometry. Increasing shear stresses (0–150 N/m<sup>2</sup>) were applied to the solutions at 20°C.

Surface tension determinations were carried out according to the Wilhelmy plate method, on Dognon-Abribat tensiometer (Prolabo, Paris, France).

**Prills characterization**

At the end of the prilling process, prill’s diameter was measured by transmission optical microscopy (Nikon Labophot, Tokyo, Japan, magnification 4) combined with a JVC video camera (JVC Americas Corp., Wayne, NJ). MediaGrabber™3.0 (Raster Ops Corp.,

Santa Clara, CA) and NIH Image 1.60 (NIH, Bethesda, MD) image processing softwares were used for image treatment. Afterwards, the prills produced were crosslinked and dried in the same conditions as described in the first part of this work. Particle size distribution, specific surface area, and true density were also determined.

**RESULTS AND DISCUSSION**

**Beads preparation**

The dosage of PEO by gel permeation chromatography revealed that PEO did not leak from the beads in the 10%(w/v) sodium hydroxide solution, but actually precipitated in those pH conditions. This means that the high molecular weight PEO chains remained trapped within CS chains during the dropping process. Through the washing step, 16% of the PEO initially introduced, leaked. Actually, the final PEO ratio was 17 ± 1%(w/w) in relation to the total weight of dried CS instead of the 20% theoretical ratio.

CS chains are crosslinked with glyoxal to build up a covalent network through the formation of a Schiff

**TABLE II**  
**Dimensions (Determined by Laser Diffraction) and Textural Parameters for CS1.5% and CS1.5% PEO Dried Beads, Obtained by the Non-Vibrating Dropping Process, Whether CS Is Crosslinked or Not (mean ± S.D.). G indicates a cross-linked CS**

	Mean diameter* (µm)	Median diameter (µm)	Mean/median ratio	True density (g/cm <sup>3</sup> )	Specific surface area (m <sup>2</sup> /g)	Textural factor
CS1.5%	741 ± 2	716 ± 1	1.03	1.4394 ± 0.0001	0.048 ± 0.004	9
CS1.5% G	587 ± 2	585 ± 1	1.00	1.4167 ± 0.0003	0.045 ± 0.003	6
CS1.5% PEO	702 ± 2	679 ± 2	1.03	1.4427 ± 0.0002	0.056 ± 0.003	9
CS1.5% G PEO	557 ± 1	556 ± 1	1.00	1.4169 ± 0.0001	0.054 ± 0.006	7

\* mean ± S.E.M.

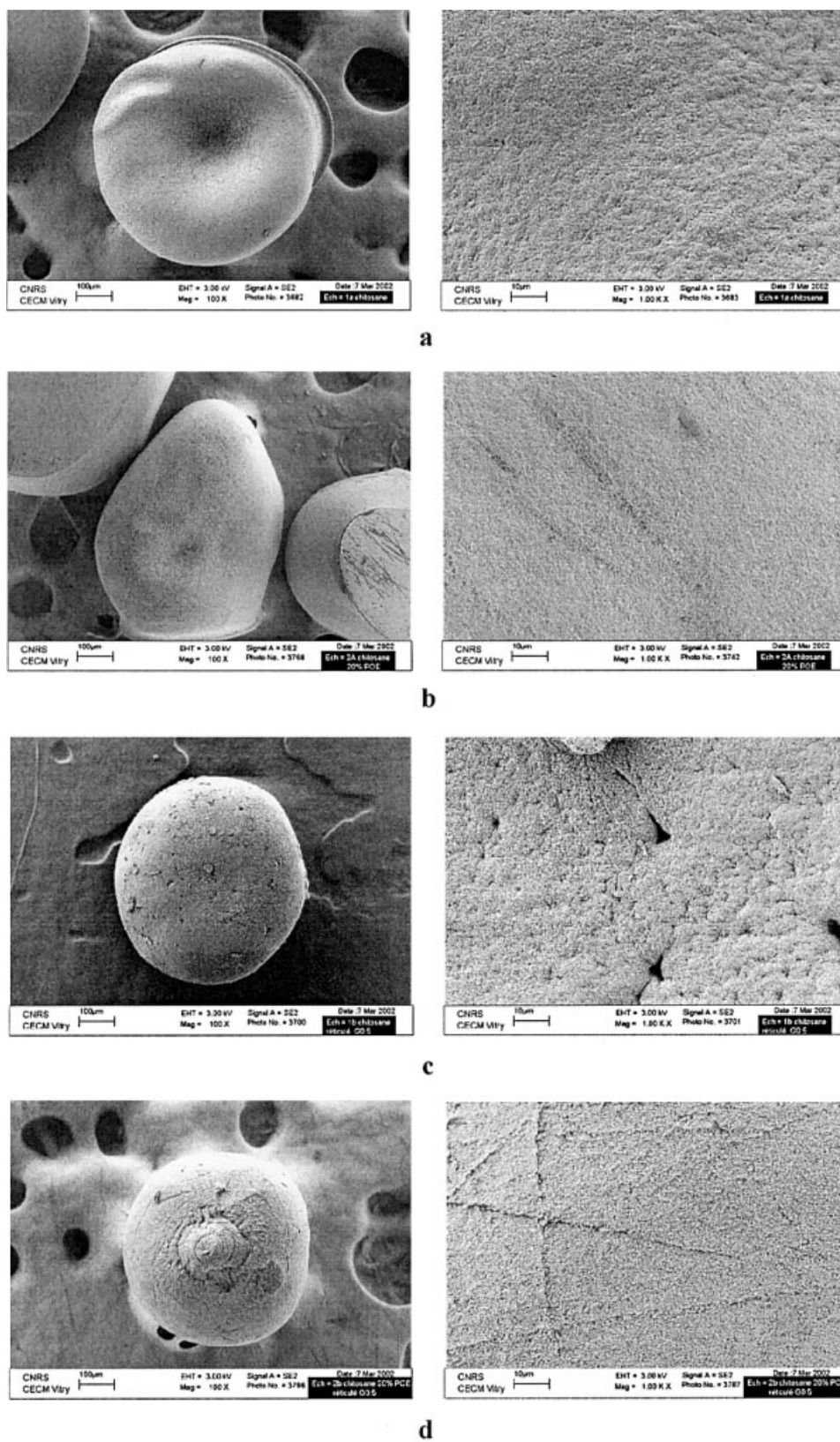


**Figure 5** SEM photographs of dried beads' shape and surface: (a) CS1.5%, (b) CS1.5% PEO, (c) CS1.5% G, and (d) CS1.5% G PEO.

base. As a result of the implication of CS amine functions into the imine functions of the Schiff base, an inversion of the ratio between the intensities of the amine (1590 cm<sup>-1</sup>) and the amide (1649 cm<sup>-1</sup>) characteristic peaks of the CS was observed on IR spectra (Fig. 3).

The amount of bound glyoxal in relation to the total amount of introduced glyoxal, allowed the determination of an effective [glyoxal : amine group] molar ratio, as indicated in Table I. The values show a quite incomplete crosslinking reaction. This may be due to the creation of a barrier against diffusion of the crosslinking agent as the reaction goes on.

Another relevant point is the estimation of the average molar mass of CS chains between two crosslinks (noted  $M_C$ ). As shown in Table I, effective [glyoxal : amine group] molar ratio appears in the form  $\alpha : 1$ , that is, 1 mol of glyoxal for  $1/\alpha$  mole of NH<sub>2</sub>. Assuming that 1 molecule of glyoxal reacts with 2 amine groups, there remain  $[(1/\alpha) - 2]$  free amine groups. According to CS average deacetylation degree, there are 83 deacetylated units (NH<sub>2</sub>) for 17 acetylated units within polymer chain. Thus, between two crosslinks, CS chain presents  $[(1/\alpha) - 2]$  deacetylated units and  $[(1/\alpha) - 2] \times 17/83$  acetylated units. So, the equation for calculation of  $M_C$  is:

$$M_C = \left(\frac{1}{\alpha} - 2\right) \times M_{DEAC} + \left(\frac{1}{\alpha} - 2\right) \times \frac{17}{83} \times M_{AC} \quad (1)$$

where  $M_{DEAC}$  and  $M_{AC}$  are the molar masses of deacetylated and acetylated units, respectively.

For both reference and semi-IPN beads, these  $M_C$  values are close to each other (Table I). This might be an indication of a quite similar structure of CS covalent networks in both systems.

**Particle size distribution and textural characterization**

Thanks to a dynamical drying process, well individualized spheroid particles could be macroscopically observed. Dried beads were analyzed in terms of size distribution by laser diffraction. All distribution profiles were single modal, with a narrower distribution for the crosslinked beads (Fig. 4). As shown in Table II, mean/median ratios indicate a more symmetrical size

distribution for crosslinked beads compared to non crosslinked ones, revealing a more homogeneous population of dried beads in the first case. The crosslinking process had an influence on the final size of dried beads. When crosslinked, beads presented a smaller diameter (Table II).

The study of textural properties showed that true density was clearly modified by the crosslinking of CS (Table II). Crosslinked CS based beads showed a decreased density that could correspond to higher porosity. This point may be surprising if we take into account the smaller size of crosslinked beads, as mentioned above. However, this could be explained by the fact that non crosslinked beads tended to collapse under drying, resulting in "red blood cell-shaped" beads (Fig. 5a and b). In this case, actually, the diameter measured by laser diffraction corresponded to the larger one. By contrast, crosslinked beads kept their spherical form; this is the reason why their diameter appeared smaller.

As indicated in Table II, semi-IPN beads have a specific surface area very close to that of CS beads. They both present a very low specific surface area. An interesting comparative parameter is the textural factor. This factor is the ratio between the specific surface area of the bead, and the specific surface area of the perfectly smooth and nonporous sphere of same mean diameter and true density. It gives an indication of the rugosity of the surface, compared to the equivalent smooth sphere. According to this textural factor, PEO did not modify beads' surface. Furthermore, crosslinking tended to intensify their smoothness. As demonstrated by the photomicrographs, crosslinking contributed to an improved roundness of the particles (Figs. 5c and d). Beads' surface appeared very smooth, justifying the low specific surface area values.

**Transposition to a prilling device**

Formulation and process parameters

Prill size depends on many factors, such as the material's density and surface tension, as well as the nozzle diameter.<sup>21</sup> These factors, together with vibration frequency, determine the size of the prills that are generated. A physical limitation to the process is given by the properties of the liquid. An example of physical

**TABLE III**  
**Cross Rheological Parameters for CS and CS / PEO Solutions With Two Different Concentrations of CS (mean ± S.D.)**

	$\mu_0$ (Pa.s)	$\mu_\infty$ (Pa.s)	$c$ (s)	$n$
CS1.5%	2.3 ± 0.2	0.07 ± 0.05	0.011 ± 0.002	0.84 ± 0.08
CS1.5% PEO	2.5 ± 0.1	0.13 ± 0.03	0.0106 ± 0.0003	0.89 ± 0.03
CS1%	0.72 ± 0.02	0.053 ± 0.006	0.0074 ± 0.0005	0.88 ± 0.03
CS1% PEO	0.84 ± 0.01	0.091 ± 0.009	0.00741 ± 0.00005	0.93 ± 0.02

TABLE IV  
Evaluated Jet Flow Parameters for CS and CS / PEO Solutions With Two Different Concentrations of CS (mean  $\pm$  S.D.)

	$\sigma$ ( $\times 10^{-3}$ N/m)	$Q$ ( $\times 10^{-9}$ m <sup>3</sup> /s)	$\dot{\gamma}$ ( $\times 10^5$ s <sup>-1</sup> )	$\mu$ (Pa.s)	$u$ (m/s)	$R_e$
CS1%	39.6 $\pm$ 0.4	117	1.5	0.055 $\pm$ 0.006	3.7	14
CS1% PEO	27.1 $\pm$ 0.3	100	1.3	0.092 $\pm$ 0.009	3.2	7
CS1.5%	46.3 $\pm$ 0.3	-	-	-	-	-
CS1.5% PEO	42.5 $\pm$ 0.6	-	-	-	-	-

limitation is the liquid pressure, which can increase with high viscosity, particularly when a small nozzle diameter is used.

Since the nozzle used had a small internal diameter (200  $\mu$ m), some parameters needed to be optimized on grounds of process feasibility.

Sakai and Hoshino demonstrated that the jet break-up phenomenon is related to the liquid speed.<sup>22</sup> For a given liquid and nozzle diameter, there is a threshold speed below which a simple drip is observed. When speed rises, a jet forms. Droplets' diameter, however, is not yet uniform. Indeed, there is another threshold speed for which coalescence between main and satellite droplets takes place, leading to uniform droplets. Moreover, to get an efficient jet break-up, the flow must be laminar.<sup>23</sup> This is characterized by a critical Reynolds number ( $R_{ec}$ ) that has to stand below a value of 2000.<sup>18</sup> A thin, regular, and laminar jet is thus required for the process.

The viscosity  $\mu$ (Pa.s) of non-newtonian CS solutions, at the shear rate  $\dot{\gamma}$ (s<sup>-1</sup>) inside the nozzle, was derived from the Cross model:<sup>24</sup>

$$\frac{\mu - \mu_\infty}{\mu_0 - \mu_\infty} = \frac{1}{1 + (c \cdot \dot{\gamma})^n} \quad (2)$$

where  $\mu_0$  and  $\mu_\infty$  are the shear viscosities for zero and infinite shear rates, respectively;  $c$ (s) and  $n$  are rheological parameters;  $\dot{\gamma}$  is calculated from the superimposed flow rate  $Q$ (m<sup>3</sup>/s) and the nozzle radius  $R$ (m):

$$\dot{\gamma} = \frac{4 \cdot Q}{\pi \cdot R^3} \quad (3)$$

Solutions with 1.5%(w/w) of CS did not succeed in circulating through the 200  $\mu$ m nozzle according to the above requirements. Their viscosity  $\mu_0$  constituted a limiting factor (Table III). Clogging of the nozzle occurred when jet speed was increased, particularly at the beginning of the process when a higher flow rate was necessary to establish the laminar jet. With such a high viscosity, the wavelength of the vibration frequency was unlikely to make possible the achievement of a thin breakable jet. That is why the percent-

age of CS in the solutions to prill was reduced to 1%(w/w).

Jet flow parameters such as surface tension  $\sigma$ (N/m), shear rate  $\dot{\gamma}$  and viscosity  $\mu$  at the flow rate  $Q$ , jet speed  $u$ (m/s), and corresponding Reynolds number  $R_e$ , are reported in Table IV.

$R_e$  is defined as:

$$R_e = \frac{\rho \cdot u \cdot d}{\mu} \quad (4)$$

where  $\rho$ (g/m<sup>3</sup>) is the solution density and  $d$ (m) the nozzle diameter.

The measured parameters for CS 1%(w/w) solutions did comply with the required quality of the jet. Speed values were satisfactory to ensure a regular prilling as well as a sufficient resistance of the beads at the impact point with the reception solution.

Uniformity of droplet size and droplets' distance depends on the amplitude of the vibration.<sup>22</sup> There is a threshold for the vibration amplitude for which size gets uniform. While further increasing this amplitude, droplets become equidistant.

Rayleigh showed that the frequency  $f$  (Hz) leading to maximum jet instability is related to jet speed  $u$  and to vibration wavelength according to the following general equation:<sup>20</sup>

$$f = \frac{u}{\lambda_R} \quad (5)$$

where  $\lambda_R$  (m) is the Rayleigh–Weber wavelength given by:<sup>25</sup>

TABLE V  
Prilling Process Parameters

Nozzle diameter ( $\mu$ m)	Average jet speed (m/s)	Vibration frequency (Hz)	Vibration amplitude (%)	Nozzle/hardening solution distance (cm)
200	3.5	300	100	30

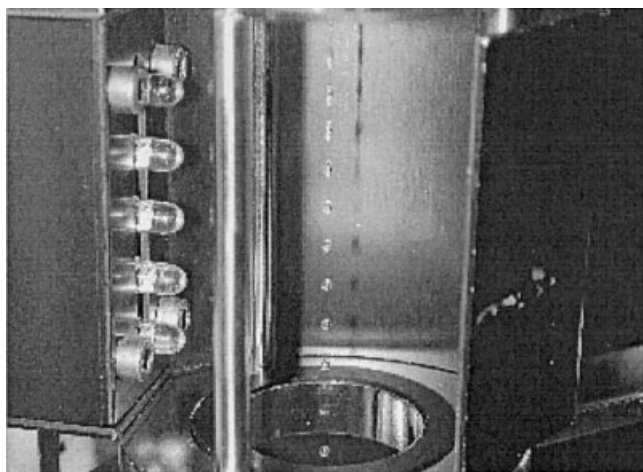


**Figure 6** Photograph of the chain of droplets visualized thanks to the LED-stroboscopic light.

$$\lambda_R = 4.5 \cdot d \cdot \left( \frac{3 \cdot \mu}{(\rho \cdot \sigma \cdot d)^{1/2}} + 1 \right)^{1/2} \quad (6)$$

with viscosity  $\mu$ , density  $\rho$ , and surface tension  $\sigma$  the solution properties, and  $d$  the nozzle diameter.

As a consequence, for a given solution and nozzle diameter, there is a range of frequencies corresponding to the droplets' size and distance uniformity zone, as a function of jet speed. As laminar flow is obtained for lower jet speeds, the lower frequency producing jet instability was chosen.

A summary of the prilling conditions is presented in Table V.

The generated drops could be observed by means of an LED-stroboscopic light as a stationary row of drops (Fig. 6). The stroboscopic light was automatically synchronized with the superimposed vibration frequency and allowed to visualize the most efficient one. Amplitude and frequency of the nozzle oscillation were held constant so that a monodisperse drop size distribution was obtained. Uniformity of droplets' size and droplets' distance was clearly observed (Fig. 6).

### Prills characterization

Prills' mean diameter was extracted from the perimeter measured on microscope. Values are reported in Table VI. Prills could be represented by spheroids,

**TABLE VI**  
Prills' Size and Shape Factor (D / d) Determined by Optical Microscopy Before Drying (mean  $\pm$  S.D.)

	Mean diameter ( $\mu\text{m}$ )	D / d
CS1%	730 $\pm$ 60 (n = 105)	1.17 $\pm$ 0.07
CS1% PEO	750 $\pm$ 40 (n = 100)	1.15 $\pm$ 0.07

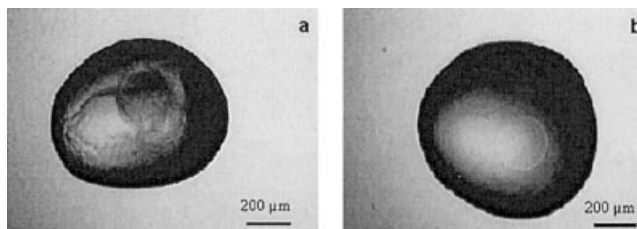


**Figure 7** Photomicrographs of (a) CS1% and (b) CS1% PEO beads obtained by prilling before drying.

characterized by a major (D) and a minor (d) diameter. A shape factor was calculated from the ratio between those two diameters. Both CS and semi-IPN prills presented a shape factor lower than 1.2, which means that they could be considered as spheres (Fig. 7).<sup>18</sup> At the stage of the prilling process, size distribution was well monodisperse.

After drying, textural studies revealed a slightly higher specific surface area for the beads produced by prilling (Table VII). This increase was due, not to a greater rugosity of the particles, but to their smaller size. Indeed, textural factor remained unchanged. The particle size distribution determined by laser diffraction presented the same characteristics as already commented for the beads produced by the nonvibrating dropping technique. The population of prills showed a single modal profile and monodispersity.

### CONCLUSION

In this study, preparation of semi-interpenetrating micro networks of chitosan/poly(ethylene oxide) could be achieved by a dropping process. As demonstrated by chromatography experiments, poly(ethylene oxide) chains remained trapped within chitosan chains inside the synthesized particles. Semi-interpenetrating systems presented a crosslinking ratio similar to that of the reference chitosan networks. The dropping of the chitosan/poly(ethylene oxide) solution, combined with a drying process of the resulting particles in a fluidized bed apparatus, led to the production of a monodisperse population of beads. Crosslinked beads were characterized by a narrower distribution profile, compared to non crosslinked ones. Furthermore, the crosslinking of chitosan chains created a network capable of keeping the spherical structure of the particles even after drying. By contrast, non crosslinked particles tended to collapse due to the low polymer content. Both chitosan network beads and semi-interpenetrating network beads presented a low specific surface area, but crosslinking still intensified the smoothness of the particles. Provided that chitosan concentration was reduced, the semi-interpenetrating micro network could be synthesized within smaller size and at a larger scale by transposition to a prilling



**TABLE VII**  
**Dimensions (determined by laser diffraction) and Textural Parameters for Crosslinked CS (CS1% G) and Semi-IPN (CS1% G PEO) Dried Beads Obtained by Prilling (mean  $\pm$  S.D.)**

	Mean diameter ( $\mu\text{m}$ )	Median diameter ( $\mu\text{m}$ )	Mean / median ratio	True density ( $\text{g}/\text{cm}^3$ )	Specific surface area ( $\text{m}^2/\text{g}$ )	Textural factor
CS1% G	341 $\pm$ 3	324 $\pm$ 2	1.05	1.4216 $\pm$ 0.0005	0.092 $\pm$ 0.001	7
CS1% G PEO	338 $\pm$ 5	325 $\pm$ 1	1.04	1.4239 $\pm$ 0.0005	0.103 $\pm$ 0.006	8

process. Technical parameters such as vibration frequency, amplitude, and solution flow rate were optimized to achieve satisfactory jet characteristics. The uniformity of droplets produced in this way could be observed macroscopically and confirmed microscopically. With a reproducible and high productivity process, prilling technique led to the generation of spherical particles whose diameter, after drying, was centered in the region of 300  $\mu\text{m}$ . Such a divided and well calibrated solid form may be useful as a drug carrier excipient for the oral delivery strategy.

The French ministry of Research is gratefully acknowledged for supporting the Franco-Italian collaboration. The authors wish to thank Mr. J.-L. Pastol from the Centre d'Etudes de Chimie Métallurgique UPR CNRS 2801 (Vitry-sur-Seine, France) for his contribution to the SEM studies.

## References

- Chandy, T.; Sharma, C. P. *Biomater Art Cells Immob Biotech* 1991, 19, 745.
- Sharma, C. P.; Rao, S. B. *J Biomed Mater Res* 1997, 34, 21.
- Muzzarelli, R. A. A. In *Chitin*, R. A. A. Muzzarelli, Ed.; Pergamon Press: Oxford, 1977.
- Shepherd, R.; Reader, S.; Falshaw, A. *Glycoconj J* 1997, 14, 535.
- Illum, L. *Pharm Res* 1998, 15, 1326.
- Hirano, S. *Polym Int* 1999, 48, 732.
- Chandy, T.; Sharma, C. P. *Biomaterials* 1993, 14, 939.
- Gupta, K. C.; Ravi Kumar, M. N. V. *Biomaterials* 2000, 21, 1115.
- Patel, V. R.; Amiji, M. M. *Pharm Res* 1996, 13, 588.
- Khalid, M. N.; Ho, L.; Agnely, F.; Grossiord, J. L.; Couarraze, G. *S T P Pharma Sci* 1999, 9, 359.
- Khalid, M. N.; Agnely, F.; Yagoubi, N.; Grossiord, J. L.; Couarraze, G. *Eur J Pharm Sci* 2002, 15, 425.
- Brugnerotto, J.; Lizardi, J.; Goycoolea, F. M.; Argüelles-Monal, W.; Desbrières, J.; Rinaudo, M. *Polymer* 2001, 42, 3569.
- Roberts, G. A. F.; Domszy, J. G. *Int J Biol Macromol* 1982, 4, 374.
- Roberts, G. A. F.; Taylor, K. E. *Makromol Chem* 1989, 190, 951.
- Hsien, T. Y.; Rorrer, G. L. *Ind Eng Chem Res* 1997, 36, 3631.
- Mitchel, R. E. J.; Birnboim, H. C. *Anal Biochem* 1977, 81, 47.
- Deleuil, M.; Labourt-Ibarre, P.; Robert, R.; Eraclis, S. (to Rhône Poulenc Santé) *Fr. Pat. FR 2657257* (1990).
- Dumas, H.; Tardy, M.; Rochat, M. H.; Tayot, J. L. *Drug Dev Ind Pharm* 1992, 18, 1395.
- Limousin, V. *Info Chimie* 1997, 389, 124.
- Rayleigh, L. *Proc Lond Math Soc*, 1878, 10, 4.
- Laurent, S.; Puiggali, J. R.; Roques, M. *Entropie* 1997, 204, 11.
- Sakai, T.; Hoshino, N. *J Chem Eng Japan* 1980, 13, 263.
- Dumas, H.; Tardy, M.; Tayot, J. L.; Rochat, M. H.; Verain, A. *Technique du prilling adaptée à des solutions de collagène*, 5th International Conference of Pharmaceutical Technology, Paris, 1989, 25.
- Soong, D.; Shen, M. *J Rheol* 1981, 25, 259.
- Weber, C. *Math Mech* 1931, 11, 136.